Interchange of Catalytic Activity within the 2-Enoyl-Coenzyme A Hydratase/Isomerase Superfamily Based on a Common Active Site Template†

Hong Xiang, Lusong Luo, Kimberly L. Taylor, and Debra Dunaway-Mariano*

Department of Chemistry, University of New Mexico, Albuquerque, New Mexico 87131

Received January 21, 1999; Revised Manuscript Received March 26, 1999

ABSTRACT: The structures and chemical pathways associated with the members of the 2-enoyl-CoA hydratase/isomerase enzyme superfamily are compared to show that a common active site design provides the members of this family with a CoA binding site, an expandable acyl binding pocket, an oxyanion hole for binding/polarizing the thioester C═O, and multiple active site stations for the positioning of acidic and basic amino acid side chains for use in proton shuttling. It is hypothesized that this active site template can be tailored to catalyze a wide range of chemical transformations through strategic positioning of acid/base residues among the active site stations. To test this hypothesis, the active site of one member of the 2-enoyl-CoA hydratase/isomerase family, 4-chlorobenzoyl-CoA dehalogenase, was altered by site-directed mutagenesis to include the two glutamate residues functioning in acid/base catalysis in a second family member, crotonase. Catalysis of the syn hydration of crotonyl-CoA, absent in the wild-type 4-chlorobenzoyl-CoA dehalogenase, was shown to occur with the structurally modified 4-chlorobenzoyl-CoA dehalogenase at $k_{cat} = 0.06\ s^{-1}$ and $K_m = 50\ \mu M$.

The development of a new enzyme catalyst in the laboratory, or in nature, relies on the modification of a preexisting protein framework to perform a new chemical task. The fact that enzymes, grouped together on the basis of common fold, are often related by similarities in the chemistries catalyzed (for a recent review see ref *1*), suggests that an active site structure may be modified to support a range of chemical transformations. In the present study we have examined the structures of the members of the 2-enoyl-CoA hydratase/isomerase superfamily of enzymes and found that they share a common active site design which supports a variety of reactions occurring on a highly polarized thioester (or amide) unit. The implication of such a highly conserved active site is that the diversity of the chemical reactions catalyzed is based on strategic positioning of catalytic groups within the active site framework. To test this idea, the active site of one member of the 2-enoyl-CoA hydratase/isomerase family (*2*, *3*), 4-chlorobenzoyl-CoA dehalogenase, was altered by site-directed mutagenesis to include the two glutamate residues functioning in acid/base catalysis in a second family member, crotonase. The dehalogenase mutant was shown to catalyze the syn hydration of crotonyl-CoA whereas wild-type dehalogenase was shown to be devoid of such activity.

EXPERIMENTAL PROCEDURES

Materials. Crotonyl-CoA, purchased from Sigma and containing 5−10% cis isomer, was used without further purification. Acetoacetyl-CoA, D,L-3-hydroxybutyryl-CoA, crotonase, and bovine albumin were purchased from Sigma. The *Escherichia coli* JM101 cells containing plasmid pT 7.5 (*4*) and expressing wild-type *Pseudomonas* sp. strain CBS3 4-CBA-CoA[1] dehalogenase were grown to mid-log phase in LB media with 50 μg of ampicillin/mL at 37 °C before being harvested. Plasmid DNA for sequencing and mutagenesis was obtained by using the QIAprep Spin Miniprep kit from QIAGEN. Primers for PCR and sequencing reactions were purchased from Life Technologies. Enzymes for DNA manipulation were purchased from Promega or New England Biolabs and used with the supplied buffers. *E. coli* BL21 (DE3) competent cells were purchased from Novagen.

Site-Directed Mutagenesis. The 4-CBA-CoA dehalogenase triple mutant A136P/W137E/D145A was constructed by PCR (*5*) using the D145A mutant gene as template and essentially the same protocol described in Yang et al. (*6*). The resulting clone was transformed into competent *E. coli* BL21 (DE3) cells for gene expression. The G117E/A136P/W137E/N144P/D145G/T146A/A147G/T148G dehalogenase mutant was constructed in two steps. First, the G117E mutant was prepared from the wild-type dehalogenase gene using the standard "overlapping " PCR method while the N144P/D145G/T146A/A147G/T148G dehalogenase mutant was prepared by the "overhang" PCR method using the A136P/W137E/D145A dehalogenase mutant gene as template. The G117E mutant and N144P/D145G/T146A/A147G/T148G mutant plasmids were digested with *Nru*I and *Bst*BI restriction enzymes. The desired DNA fragments were purified by agarose gel chromatography and then ligated using T4 DNA ligase. The resulting clone was transformed into competent

† This research was supported by NIH Grant GM28688.

* To whom correspondence should be addressed. Phone: 505-277-3383. Fax: 505-277-2609. E-mail: dd39@unm.edu.

[1] Abbreviations: 4-CBA, 4-chlorobenzoate; 4-CBA-CoA, 4-chlorobenzoyl-coenzyme A; 4-HBA-CoA, 4-hydroxybenzoyl-CoA; DTT, dithiothreitol; Hepes, *N*-(2-hydroxyethyl)piperzine-*N*′-2-ethanesulfonic acid; HPLC, high-performance liquid chromatography; FPLC, fast protein liquid chromatography; NMR, nuclear magnetic resonance.

10.1021/bi9901432 CCC: $18.00
Published on Web 05/26/1999

E. coli BL21 (DE3) cells for gene expression. The G117A/A136P/W137E/N144P/D145G/T146A/A147G/T148G dehalogenase, G117D/A136P/W137E/N144P/D145G/T146A/A147G/T148G dehalogenase, and G117E/A136P/W137D/N144P/D145G/T146A/A147G/T148G dehalogenase mutants were constructed using the same general method used to construct the G117E/A136P/W137E/N144P/D145G/T146A/A147G/T148G dehalogenase mutant. The sequence of each mutant was verified by commercial DNA sequencing (Center for Agricultural Technology, University of Maryland).

Purification of Wild-Type and 4-CBA-CoA Dehalogenase Mutants. The G117A/A136P/W137E/N144P/D145G/T146A/A147G/T148G dehalogenase and G117D/A136P/W137E/N144P/D145G/T146A/A147G/T148G dehalogenase mutants proved to be too unstable to be isolated. The wild-type dehalogenase was purified by the method described in Liang et al. (*7*). The purification of the A136P/W137E/D145A dehalogenase mutant was carried out by using the same protocol described in Yang et al. (*6*) for the H90Q dehalogenase mutant. The purifications of the G117E/A136P/W137E/N144P/D145G/T146A/A147G/T148G and G117E/A136P/W137D/N144P/D145G/T146A/A147G/T148G dehalogenase mutant proteins were carried out by using a modification of this procedure wherein the DEAE-cellulose column fractions containing the mutant dehalogenase were concentrated and purified using a Pharmacia FPLC equipped with a Superose 12 column with 50 mM K^+Hepes, pH 7.5/0.15 M NaCl/1 mM DTT serving as eluant (0.5 mL/min). The respective yields of the mutant dehalogenases are: 100, 50, and 40 mg of pure (based on SDS−PAGE analysis) protein/25 g of wet cell paste.

Enzyme Assays. 4-CBA-CoA dehalogenase catalysis of 4-CBA-CoA dehalogenation to 4-HBA-CoA in 50 mM K^+-Hepes buffer (pH 7.5, 25 °C) was assayed using the spectrophotometric-based continuous assay ($\Delta\epsilon = 8200$ M^{-1} cm^{-1} at 300 nm) described in Liang et al. (*7*). Catalysis of the hydration of crotonyl-CoA to 3-hydroxybutyryl-CoA in 44 mM Tris-HCl, 0.0044% albumin, and 0.67 mM EDTA buffer (pH 7.5, 25 °C) was assayed using the spectrophotometric-based continuous assay ($\Delta\epsilon = 3600$ M^{-1} cm^{-1} at 280 nm) described in ref 8 or using the HPLC-based fixed-time assay described here. A Rainin Dynamax HPLC system equipped with a reversed-phase C-18 column (Beckman Ultrasphere; 4.6 × 250 mm) was used to separate crotonyl-CoA from 3-hydroxybutyryl-CoA (detected at 260 nm using a UV monochromator) from protein-free reaction solutions generated by the addition of 10 μL of 0.6 N HCl to a 50 μL sample of the reaction solution (to stop the reaction), followed by the addition of 80 μL of CCl_4 with vigorous mixing (vortex) and centrifugation (to remove precipitated protein). A linear methanol gradient (30%−80% solvent B in 10 min and hold at 80% solvent B for 5 min) was employed to elute the column preequilibrated in 30% solvent B and 70% solvent A at a flow rate of 1 mL/min. Solvent A is 0% methanol and 10 mM K^+P_i (adjusted to pH 6.5 with H_3PO_4), and solvent B is 40% methanol and 10 mM K^+P_i (adjusted to pH 6.5 with H_3PO_4). The retention times of 3-hydroxybutyryl-CoA and crotonyl-CoA were 8.2 and 12.2 min, respectively.

Steady-State Kinetic Measurements. The steady-state kinetic constants V_m and K_m were measured for the G117E/A136P/W137E/N144P/D145G/T146A/A147G/T148G dehalogenase mutant catalyzed hydration of crotonyl-CoA to 3-hydroxybutyryl-CoA in 44 mM Tris-HCl, 0.0044% albumin, and 0.67 mM EDTA buffer (pH 7.5, 25 °C) using the continuous spectrophotometric assay to monitor reaction velocity. Initial velocities, measured at varying crotonyl-CoA concentrations (22−322 μM) in the presence or absence of inhibitor (245 μM acetoacetyl-CoA), were analyzed using eq 1 or 2 and the programs of Cleland (*9*).

$$V_o = V_m[A]/(K_m + [A]) \quad (1)$$

$$V_o = V_m[A]/[K_m(1 + [I]/K_i) + [A]] \quad (2)$$

where [A] is the substrate concentration, [I] is the inhibitor concentration, V_o is the initial velocity, V_m is the maximum velocity, K_m is the Michaelis constant, and K_i is the inhibition constant. The k_{cat} was calculated from the V_{max} and the enzyme subunit concentration [based on the Bradford protein determination (*10*)] used in the reaction.

Catalysis by the dehalogenase mutants A136P/W137E/D145A and G117E/A136P/W137D/N144P/D145G/T146A/A147G/T148G was monitored using the HPLC-based fixed-time assay. The G117E/A136P/W137D/N144P/D145G/T146A/A147G/T148G (25 μM) and A136P/W137E/D145A dehalogenase mutants (80 μM) were incubated with 800 μM crotonyl-CoA in 44 mM Tris-HCl, 0.0044% albumin, and 0.67 mM EDTA buffer (pH 7.5, 25 °C). Aliquots were removed at 30 s or 1 min intervals, quenched, and subjected to HPLC analysis. The initial reaction velocity was calculated from the slope of the plot of 3-hydroxybutyryl-CoA (product) concentration vs reaction time. The minimum value of k_{cat} for the reaction was calculated from the initial velocity.

UV−Visible Difference Spectral Measurements. UV−visible difference spectra of enzyme−ligand complexes were measured at 25 °C using 1 mL quartz tandem cuvettes in conjunction with a Beckman DU7400 spectrophotometer. Reference spectra were measured using 0.5 mL of 50 μM enzyme in 50 mM K^+Hepes/1 mM DTT (pH 7.5) in one compartment and 0.5 mL of 200 μM ligand in 50 mM K^+-Hepes/1 mM DTT (pH 7.5) in the other compartment. The reference spectrum was subtracted from the spectrum measured after the contents of the two compartments were mixed to give the difference spectrum. The molar extinction coefficient at the λ_{max} was calculated from the absorbance at this wavelength divided by the 25 μM enzyme subunit concentration (saturation of enzyme by ligand is assumed).

^{1}H NMR Spectral Measurements. All ^{1}H NMR spectra were measured with a Bruker DRX 500 MHz NMR spectrometer using D_2O as solvent and a probe temperature of 24−26 °C. The chemical shift data are reported with respect to the external reference 3-(trimethysilyl)propanesulfonic acid. The crotonyl-CoA triplet at 2.43 ppm (t, 2H) assigned to the two protons at 6″ on the pantetheine backbone of CoA (*11*) was used as the internal chemical shift standard as described in ref *12*. The G117E/A136P/W137E/N144P/D145G/T146A/A147G/T148G dehalogenase mutant was prepared for the reaction with crotonyl-CoA in D_2O solvent by first dialyzing a 1 mL sample enzyme ($A_{280} = 12$ ODU) dissolved in 50 mM K^+Hepes/1 mM DTT (pH 7.5) against 1 L of 50 mM KH_2PO_4 (pH 7.5) for 2 h. Six milliliters of 50 mM phosphate in D_2O (pD 7.5) was added to the enzyme sample contained in a centrifugal protein concentrator. The

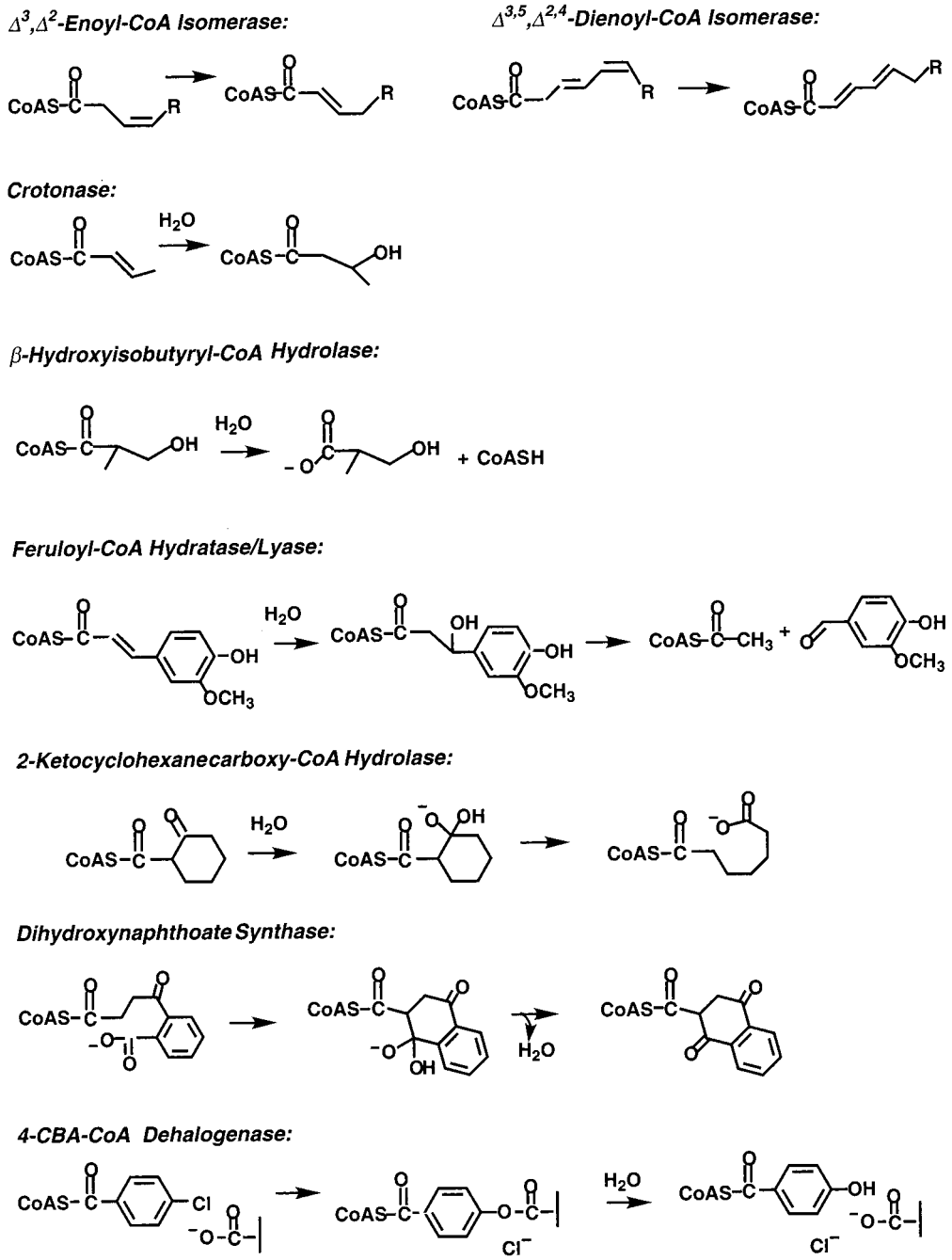

FIGURE 1: Compilation of the known reactions catalyzed by the members of the enoyl-CoA enzyme superfamily.

solution volume was reduced to 2 mL by centrifugation. This process was repeated twice more. Stock solutions of H_2O-free crotonyl-CoA were prepared as described in ref *12* whereas stock solutions of H_2O-free crotonase were prepared by dissolving bovine liver crotonase powder (370 units/mg) purchased from Sigma in D_2O (pD 7.5, 50 mM phosphate). The reaction samples were analyzed after the enzyme had been removed using a Nanosep 10K centrifugal concentrator (14 000 rpm for 15 min), and the filtrate was lyophilized to dryness and then resuspended in 50 mM phosphate buffer (pD 7.5) in D_2O.

RESULTS AND DISCUSSION

Analysis of the 2-Enoyl-CoA Enzyme Family. Evidence of a Common Active Site Structure. The 2-enoyl-CoA family of enzymes includes 4-CBA-CoA dehalogenase (*13*−*15*), 2-enoyl-CoA hydratase (crotonase) (*16*), carnitine racemase (*17*),[2] dihydroxynaphthoate synthase (*18*, *19*), 2-ketocyclo-

[2] Carnitine racemase is encoded by the *CaiE* gene of the *cai* operon necessary for carnitine metabolism in *E. coli* (*62*). The reaction catalyzed by the *CaiE* gene product is responsible for the production of D-carnitinyl-CoA; however, the substrate and thus the reaction pathway have not yet been identified. Given that the *CaiE* gene product shares 30% sequence identity with crotonase which, in turn, catalyzes the syn addition of a water molecule across the *si* face of *trans*-2-butenyl-CoA (crotonyl-CoA), we suggest that the *CiaE* gene product catalyzes the syn hydration of *cis*-crotonobetainyl-CoA to produce D-carnitinyl-CoA. Thus, in analogy to the 3-hydroxyacyl-CoA epimerase activity, the sum of the actions of two 2-enoyl-CoA hydratases of opposite stereospecificities (*63*), the *CaiE* gene product may be one hydratase of a two-hydratase system. Alternate pathways starting with other substrates can also be envisioned and thus, in the absence of a defined reaction sequence, we excluded carnitine racemase from the list represented in Figure 1.

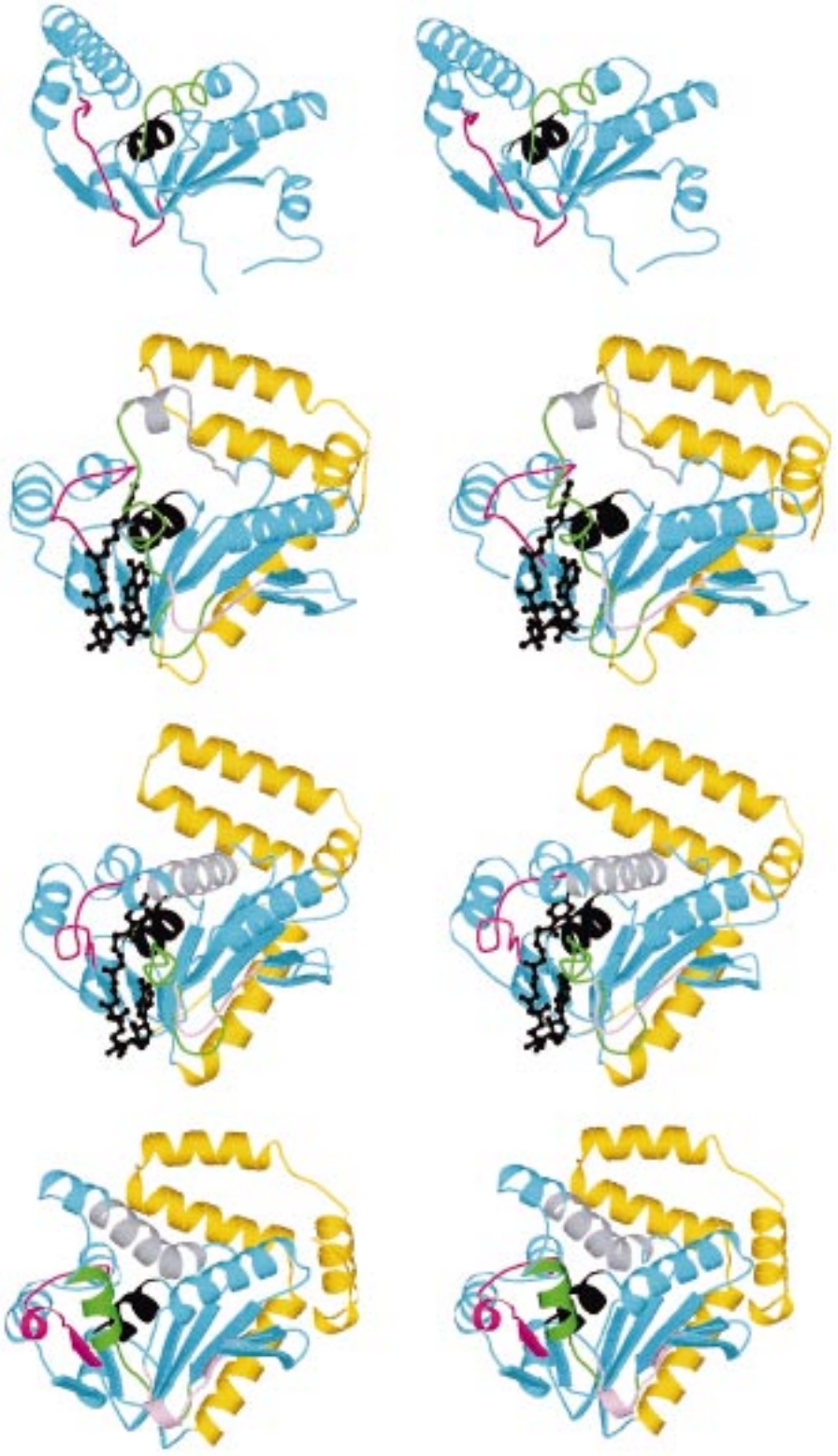

FIGURE 2: Comparison (stereoview) of the backbone folds derived from the X-ray crystal structures of (*E. coli*) apo Clp protease (*27*), (rat) crotonase complexed with the inhibitor acetoacetyl-CoA (*30*), (*Pseudomonas*) 4-CBA-CoA dehalogenase complexed with its product ligand 4-HBA-CoA (*29*), and (rat) apo $\Delta^{3,5},\Delta^{2,4}$-dienoyl-CoA isomerase (*28*) (structures are listed from top to bottom). For the three acyl-CoA enzymes, the N-terminal catalytic domain is represented in blue and the C-terminal subunit−subunit binding subdomain in yellow. The 4-HBA-CoA and acetoacetyl-CoA ligands are shown in black. The active site regions colored pink (segment 5), green (segment 2), gray (segment 4), magenta (segment 3), and black (segment 1) in three of the enzymes are described in the text. The crotonase, dehalogenase, and Clp protease ribbon diagrams were generated from the deposited coordinates using the software package Molscript (*67*). The dienoyl-CoA isomerase ribbon diagram was adapted from Modis et al. (*28*).

hexanecarboxyl-CoA hydrolase (*20*), β-hydroxyisobutyryl-CoA hydrolase (*21*, *22*), Δ^3,Δ^2-enoyl-CoA isomerase (*23*), $\Delta^{3,5},\Delta^{2,4}$-dienoyl-CoA isomerase (*24*), feruloyl-CoA hydratase/lyase (*25*), and the proteolytic component of ATP-dependent Clp protease (*26*). With the exception of the Clp protease, which catalyzes the hydrolysis of an amide linkage

in a protein substrate, each of these enzymes catalyzes a reaction at the acyl-thioester unit of an acyl-CoA substrate (see Figure 1). The Δ^3,Δ^2-enoyl-CoA isomerase and $\Delta^{3,5},\Delta^{2,4}$-dienoyl-CoA isomerase catalyze the isomerization of a double bond into conjugation with the thioester C═O by deprotonation at C(2) and protonation at C(4) or C(6), respectively. Crotonase catalyzes the reversible hydration of the C(2)═C(3) moiety in crotonyl-CoA. Feruloyl-CoA hydratase/lyase catalyzes the hydration of the C(2)═C(3) bond in the first reaction step and then the cleavage of the HC(2)−C(3)OH bond in the second step. β-Hydroxyisobutyryl-CoA hydrolase catalyzes thioester hydrolysis, while 2-ketocyclohexanecarboxyl-CoA hydrolase catalyzes hydrolytic carbon−carbon σ bond cleavage. Dihydroxynaphthoate synthase catalyzes a Claisen condensation between C(2) and the carboxyl substituent of 4-(2′-carboxyphenyl)-4-oxobutyryl-CoA in the first step, followed by elimination of hydroxide from the C(3) *gem*-diol intermediate in the second step (essentially the reverse of the 2-ketocyclohexanecarboxyl-CoA hydrolase reaction).

The seemingly wide varieties of chemistries represented by the 2-enoyl-CoA enzyme superfamily (viz., proton shuttle, amide or thioester hydrolysis, Michael addition, Claisen condensation/dehydration, Michael addition/retro Cannizzaro and nucleophilic aromatic substitution) are catalyzed by enzymes divergent in amino acid sequence but closely related in backbone fold, as evidenced by X-ray structural analysis. In Figure 2, the monomers of the four known structures, *E. coli* apo Clp protease (*27*), rat apo $\Delta^{3,5},\Delta^{2,4}$-dienoyl-CoA isomerase (*28*), *Pseudomonas* sp. strain CBS3 4-CBA-CoA dehalogenase complexed with its product ligand 4-hydroxybenzoyl-CoA (4-HBA-CoA) (*29*), and rat crotonase complexed with the inhibitor acetoacetyl-CoA (*30*), are represented. The N-terminal core (catalytic) domain of each monomer is illustrated in blue, and the C-terminal subunit−subunit binding subdomain is illustrated in yellow. The active site regions are identified by the bound ligand (shown in black) and/or by the backbone segments colored pink, magenta, green, gray, and black. The similarity in fold observed for these four, juxtaposed enzyme structures is suggestive of their common ancestry.

Active 4-CBA-CoA dehalogenase is a trimer (shown in Figure 3) while crotonase and $\Delta^{3,5},\Delta^{2,4}$-dienoyl-CoA isomerase are both dimers of trimers and the Clp protease is a tetradecamer composed of two rings of seven subunits each. The C-terminal helix−turn−helix subdomain of the dehalogenase, crotonase, and dienoyl-CoA isomerase functions in conjunction with one edge of the catalytic domain to bind the subunits together. The protease monomer, which does not have the helical C-terminal subdomain observed in the other structures, binds to a second monomer using a protruding α/β unit as a "handle" (*27*). The protease is the most distant member of the family both in the reaction that it catalyzes and in its truncated structure.

Common to the dehalogenase, crotonase, and dienoyl-CoA isomerase and to the other defined members of the enzyme superfamily (with the exception of the Clp protease) is the acyl-CoA binding site, observed in these first three enzymes at the subunit−subunit interface (see for example the ligand binding region in the dehalogenase trimer shown in Figure 3). The acyl-CoA ligand binds at this interface in the three representative enzymes with the nucleoside moiety inserted into a shallow crevice, the acyl-thioester moiety inserted into a deep, connecting crevice and the pyrophosphate−pantenoate moieties pinned onto the protein surface spanning the two crevices. While the nucleoside and pantenoate moieties form H-bonds with the enzyme residues of the two binding crevices, the phosphoryl/pyrophosphoryl moieties bind to the protein surface through ion pairs made with Arg or Lys residues. One of these ion pairs is formed with a loop residue contributed from the C-terminal subunit−subunit binding subdomain of the "B" subunit (labeled segment 6 in Figure 3), while the other two ion pairs are formed with residues from two loops contributed by the N-terminal core (catalytic) domain of subunit "A" (see the pink and green segments of Figure 2). The acyl-thioester moiety is bound entirely by residues of subunit A.

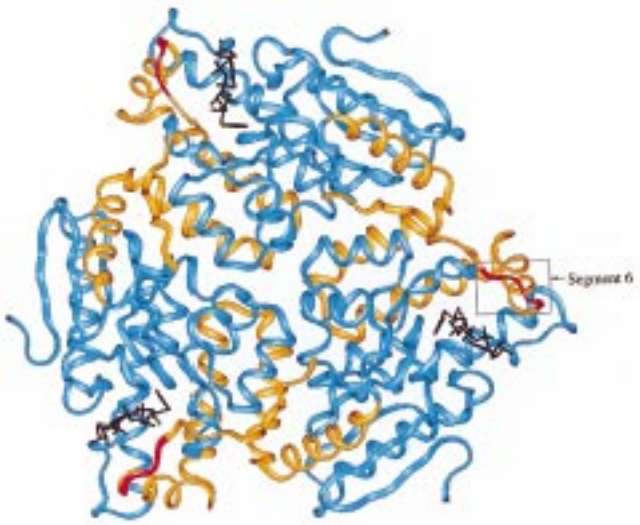

FIGURE 3: Trimeric structure of 4-CBA-CoA dehalogenase complexed with the 4-HBA-CoA ligand (*29*) generated using the modeling software package InsightII. The N-terminal catalytic domain is represented in blue and the C-terminal subunit−subunit binding subdomain in yellow. Segment 6 (see text) is shown in red and the ligand in black.

Figure 4 shows monomer cross sections, comparing the architecture of the dehalogenase and crotonase acyl-CoA ligand binding regions. The residues colored blue are the positively charged residues which serve to anchor the CoA moiety via interactions with one of the three phosphoryl groups and the side chains of the residues colored red are involved in catalyzing the respective reactions occurring at the ligand acyl moiety while the backbone amide NHs of the residues colored yellow form H-bonds with the thioester C═O of the bound ligand. The conformations of the enzyme-bound acyl-CoA ligands represented in Figure 4 [see also the NMR structural analysis of the ligand conformation described in Wu et al. (*31*)] are almost identical. The two sets of binding/catalytic residues, represented below the monomer structures in Figure 4, reflect the symmetry which exists between the functional elements of the two active sites.

Figure 5 shows the isolated segments (numbered 1−6) of the dehalogenase and crotonase active site, color-coded to match the segments illustrated in the monomer structures represented in Figure 2. From Figure 5, it is evident that five out of the six backbone segments (viz., 1, 2, 3, 5, and 6) contributing to the dehalogenase and crotonase active sites are highly conserved.[3] The same holds true for the active

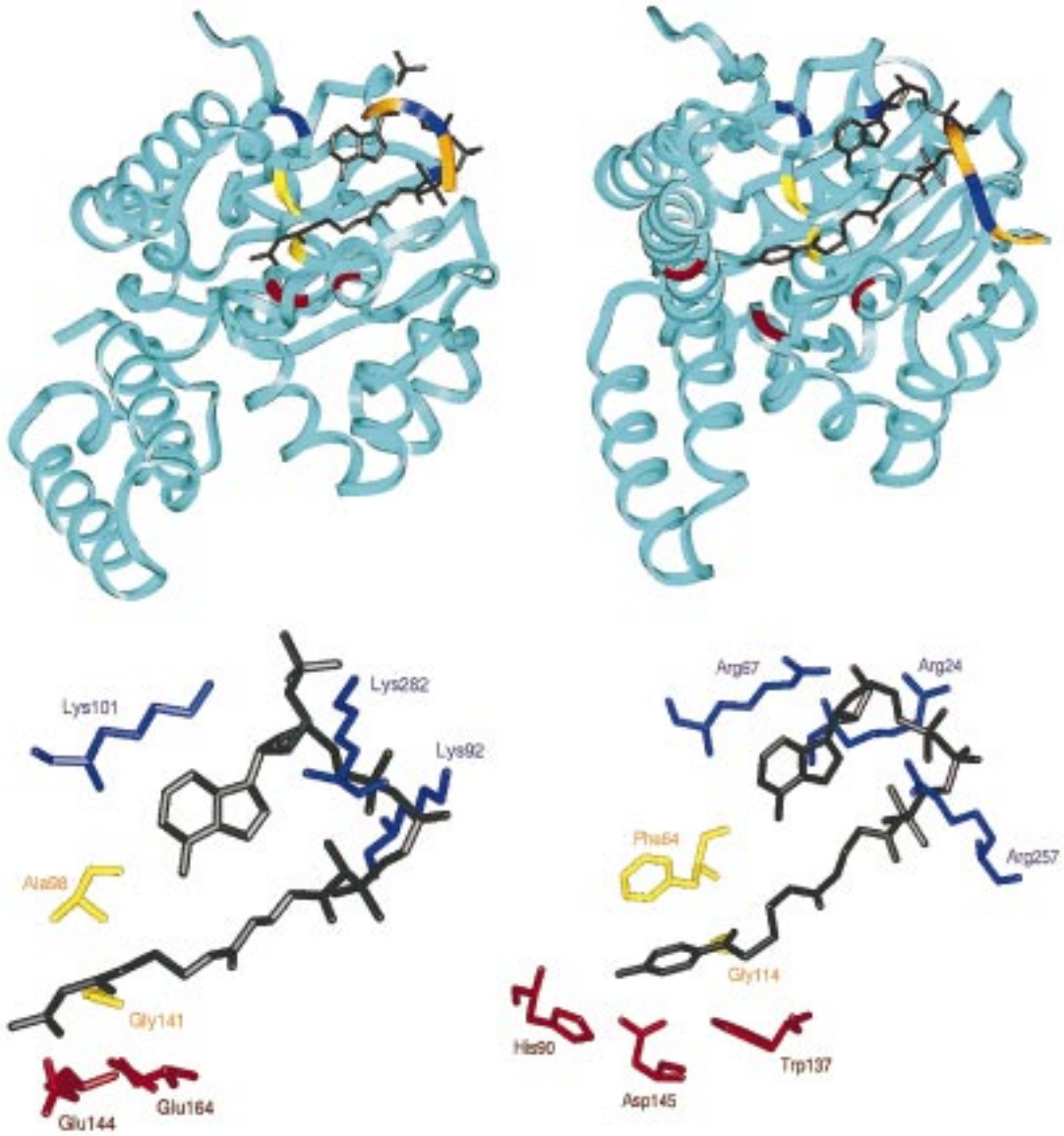

FIGURE 4: Cross sections of the active sites derived from the X-ray crystal structures of (rat) crotonase complexed with the inhibitor acetoacetyl-CoA (*30*) (left) and (*Pseudomonas*) 4-CBA-CoA dehalogenase complexed with its product ligand 4-HBA-CoA (*29*) (right) generated using the modeling software package InsightII. The CoA phosphoryl/pyrophosphoryl binding residues are shown in blue, the thioester C═O polarizing residues in yellow, and the residues functioning in acid/base catalysis in red. The ligands are shown in black.

site of the $\Delta^{3,5},\Delta^{2,4}$-dienoyl-CoA isomerase (*28*), which for lack of published coordinates is not shown. The positions on the active site segments that are within potential interaction range of a substrate ligand are indicated in Figure 5 by spheres, labeled with lower case letters. In all four enzymes represented in Figure 2, the substrate acyl C═O is polarized for catalysis through interaction with a stringently conserved oxyanion binding pocket formed by segments 1 (black) and 2 (green). In addition to participating in a dipole−dipole interaction with the positive pole of the α-helix of segment 1, the C═O forms H-bonds with the backbone NHs contributed from the residues occupying position b of segment 1 and position g of segment 2 (represented by yellow spheres in Figure 5). The catalytic residues functioning in acid/base or nucleophilic catalysis are found on segments 1−4. The Glu catalytic groups (E144 and E164) used by crotonase for the concerted, syn addition of a water molecule across the *si* face of *trans*-crotonyl-CoA (Figure 6) are located at segment 1, position e, and segment 3, position e (represented by red spheres in Figure 5).[4] The three catalytic groups of the dehalogenase, Trp137 (acid), Asp145 (nucleophile), and His90 (base) illustrated in the catalytic mechanism shown in Figure 6, are located on segment 3, positions e and m, and segment 4, position j, as pictured in Figure 5. The $\Delta^{3,5},\Delta^{2,4}$-dienoyl-CoA isomerase Glu196 and Asp204 functioning in 3-*trans*,5-*cis*-octadienoyl-CoA C(2)H deprotonation and C(6) protonation (Figure 6), respectively,

[3] Segment 4, the most variable section of the 2-enoyl-CoA enzyme family active site, forms the back wall of the active site in the liganded dehalogenase and apo-$\Delta^{3,5},\Delta^{2,4}$-dienoyl-CoA isomerase structures (Figure 2) but assumes a flexible loop conformation in the liganded crotonase structure, allowing the acyl tail of the substrate ligand to pass through the active site into intertrimer space (*64*).

[4] An alternative way to represent this reaction involves the participation of Glu144 and Glu164, both ionized, in the binding and delivery of the water molecule across the C(2)═C(3). To our knowledge, a clear distinction between these two possible mechanisms has not been experimentally demonstrated.

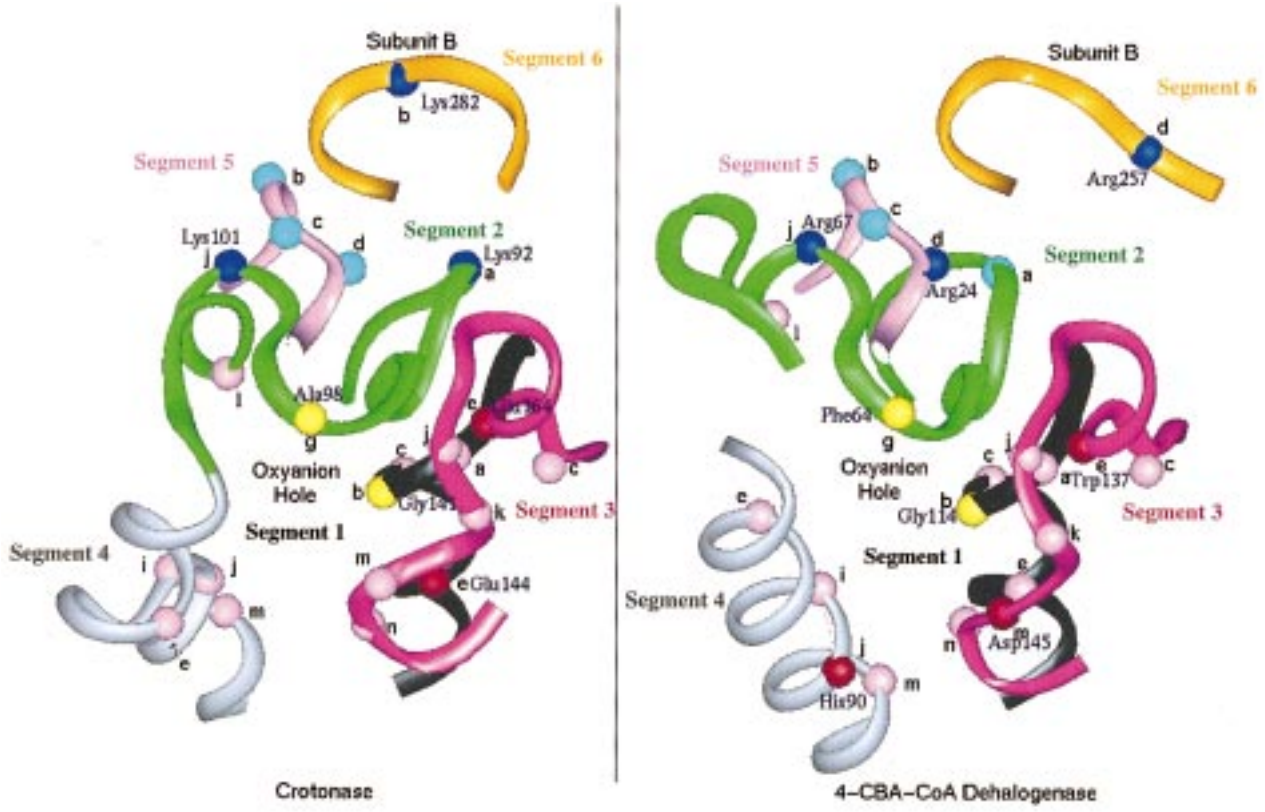

FIGURE 5: Active site region of crotonase derived from the X-ray crystal structure of the enzyme complexed with the inhibitor acetoacetyl-CoA (*30*) (left) and the active site region of 4-CBA-CoA dehalogenase derived from the X-ray crystal structure of the enzyme complexed with the product ligand 4-HBA-CoA (*29*) (right). The structural representations were generated using InsightII. The positions of the CoA phosphoryl/pyrophosphoryl binding residues are shown by dark blue spheres, the positions of the thioester C═O polarizing residues are shown by yellow spheres, and the positions of the residues functioning in acid/base or nucleophilic catalysis are shown by red spheres. The light blue spheres represent positions which are potentially within reach of a CoA phosphoryl/pyrophosphoryl group while the pink spheres represent positions which could potentially direct a side chain into the active site for interaction with the acyl moiety of the substrate ligand.

are located on segment 3, positions e and m. In the Clp protease, the Ser97 stationed at position a of segment 1 functions as the nucleophile while His122, which functions as the general base, is stationed at position k of segment 3. To anchor the CoA moiety of the substrate ligand, the dehalogenase, crotonase, and $\Delta^{3,5},\Delta^{2,4}$-dienoyl-CoA isomerase use positively charged residues located on segments 2, 5, or 6 (illustrated in Figure 5 with blue spheres).[5]

On the basis of the structural descriptions made above, one might view the active sites of the enzymes represented in Figure 2 as derivatives of a single active site structure that provides a CoA binding site (segments 2, 5, and 6), an oxyanion pocket for binding and polarizing the acyl-thioester C═O (necessary for each of the reactions shown in Figure 1; segments 1 and 2), and an expandable (via segment 4)[3] chamber containing numerous stations (located on segments 1−4) at which substrate binding and catalytic groups can be strategically positioned. To evaluate this proposal, we examined the other members of the 2-enoyl-CoA family, whose structures have not yet been reported, to see if likely catalytic groups occurred at sequence positions corresponding to the active site stations identified in Figure 5. Accordingly, the residues at the various active site stations were identified from the sequence correlations shown in Figure 7. The sequence correlations were, in turn, generated from the alignment of the family sequences with the aid of stringently conserved residues within and around the six active site segments. We discovered, using the specific residues corresponding to the active site stations and the logical chemical pathway for the catalyzed transformation (Figure 1), that reasonable models for the catalytic mechanisms can be constructed. For instance, in the case of carnitine racemase, the two Glu residues (E147 and E167) at the catalytic stations marked "e" on segments 1 and 3 and the Asp residue (D175) located at the catalytic station marked "m" on segment 3 can account for catalysis as well as the binding of the

[5] On the basis of our analysis of the 4-CBA-CoA dehalogenase (*Pseudomonas* sp. strain CBS3) and (rat) crotonase X-ray crystal structures, we have identified segment 5, positions b, c, and d, segment 2, positions a and j, and segment 6, position b or d, as possible stations for a Lys or Arg residue to make contact with the CoA phosphoryl or pyrophosphoryl moieties. The X-ray crystal structure of the *Pseudomonas* sp. strain CBS3 4-CBA-CoA dehalogenase shows that the CoA phosphate groups are bound by Arg residues located on segments 5 (position d), 2 (position j), and 6 (position d). An alignment of the three known dehalogenase sequences [*Pseudomonas* sp. strain CBS3 (*3*), *Alcaligenes* sp. strain AL3007 (*65*), and *Arthrobacter* sp. strain SU (*66*)] reveals the same use of CoA binding stations for the *Alcaligenes* dehalogenase but different use of stations for the *Arthrobacter* dehalogenase. Specifically, CoA binding is presumed to possibly occur through interaction with a Lys residue at segment 5, position c, and a Lys residue at segment 6, position b. Examination of the rat crotonase X-ray crystal structure reveals CoA phosphoryl/pyrophosphoryl moiety binding to occur with Lys residues stationed at segment 2, positions a and j, and segment 6, position b. In 3 of the 11 crotonase sequences a Glu residue is found at position b, segment 6. Likewise, in roughly half of the crotonases only one of the two segment 2 positions, a or j, carries a positively charged residue for CoA binding. Thus, within a given subfamily considerable variation in how the CoA phosphoryl/pyrophosphoryl binding stations are utilized exists.

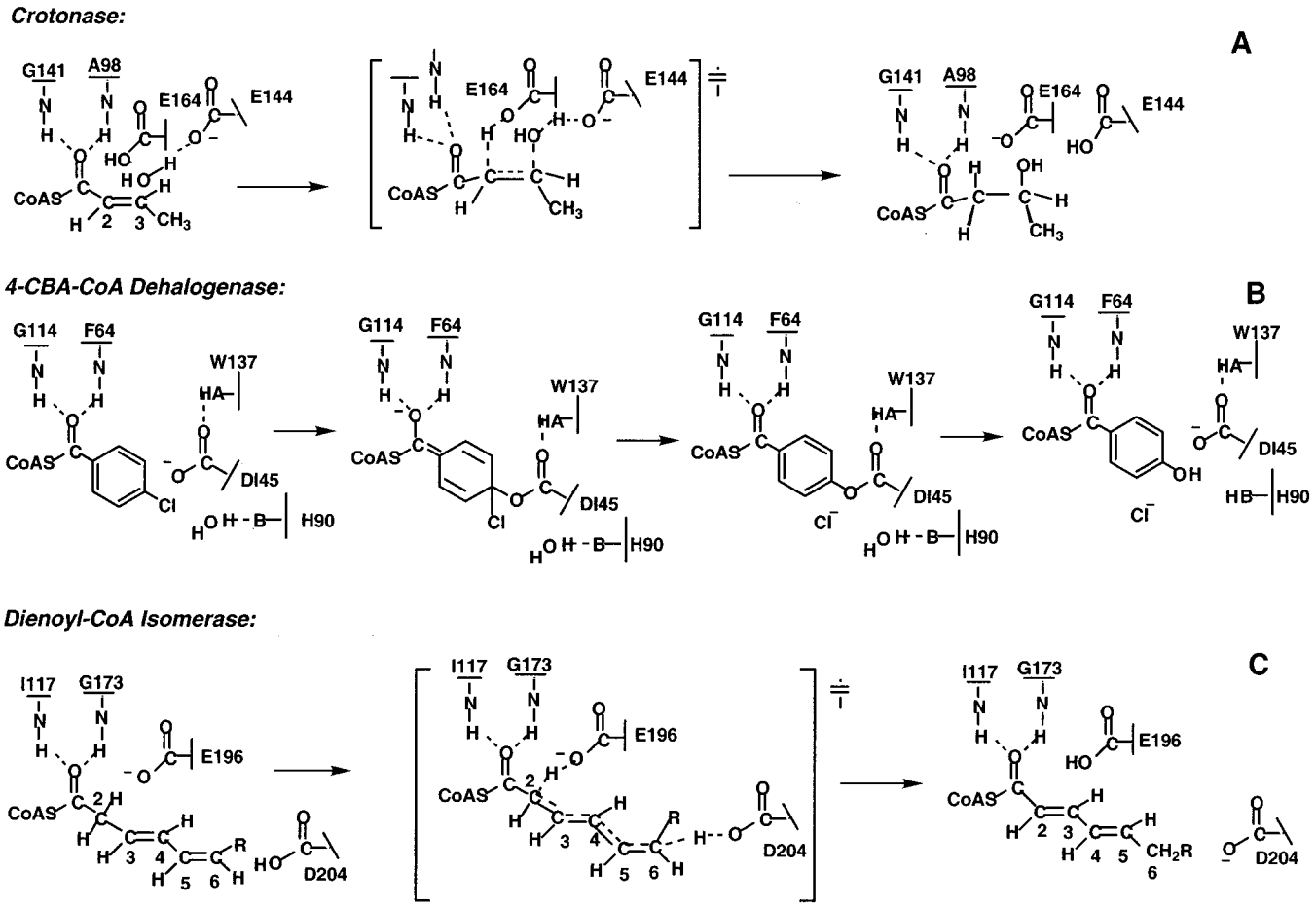

FIGURE 6: Proposed catalytic mechanisms of crotonase, 4-CBA-CoA dehalogenase and $\Delta^{3,5},\Delta^{2,4}$-dienoyl-CoA isomerase. (A) The mechanism of the crotonase reaction involves the concerted, syn addition (*42*) of a proton from Glu164 to C(2) and hydroxide from water bound to Glu144 to C(3) across the *si* face of the crotonyl-CoA C(2)═C(3) (*8, 12, 31, 33, 67*−*70*).[4] (B) The 4-CBA-CoA dehalogenase catalyzes a multistep reaction in which Asp145 adds to the benzoyl ring C(4) of the 4-CBA-CoA substrate ligand forming a Meisenhiemer intermediate (*6, 34, 35, 71, 72*). The departure of Cl^- from the ring forms the arylated intermediate which is subsequently hydrolyzed at the acyl C═O using His90 to activate the attacking water molecule and Trp137 to activate the carbonyl. (C) The mechanism of the $\Delta^{3,5},\Delta^{2,4}$-dienoyl-CoA isomerase involves the abstraction of the *pro-R* C(2) proton (*73*) by Glu196 and transfer of a solvent-derived proton (*24*) by Asp204 to C(6) in 3-*trans*,5-*cis*-dienoyl-CoA. In the crotonase, dienoyl-CoA isomerase, and 4-CBA-CoA dehalogenase active sites, the substrate ligand is activated for conjugate addition through the polarization of e^- density away from the reaction center via H-bonds formed between two backbone amide NHs and the thioester C═O (*12, 34, 35, 28*).

substrate ammonium substituent (irrespective of whether a hydratase- or an aldolase-type mechanism is involved).[2] The β-hydroxyisobutyryl-CoA hydrolase, on the other hand, has two carboxylate residues (E163 and D171) located on segment 3, positions e and m, to function in base catalysis and substrate binding while the feruloyl-CoA hydratase/lyase has a Glu residue (E143) located on segment 3, position e, and a Ser residue (S123) on segment 1, position e, as well as numerous polar residues located at key positions on segment 4, which can be incorporated into a reasonable catalytic mechanism. The Δ^3,Δ^2-enoyl-CoA isomerase contains an essential Glu residue (E165) (*32*) stationed on segment 3, position e, for acid/base catalysis. 2-Ketocyclohexanecarboxyl-CoA hydrolase and dihydroxynaphthoate synthase, on the other hand, have both a Ser residue located on segment 3, position j, and several other polar residues located on segments 2 and 4 to function in acid/base catalysis and substrate binding.[6] In all cases, at least one of the potential CoA binding stations identified on segments 2, 5, and 6 (see Figure 5) is filled by a Lys or Arg residue. Once the X-ray crystal structures of these additional family members are solved, the extent to which the active site design observed in the present structures is conserved throughout the entire family will be known. For now, however, we are almost certain that these active site structures will adhere to the general template structure.

Assuming that the active site oxyanion and CoA binding pockets as well as the catalytic stations are conserved among the 2-enoyl-CoA family members, we concluded that the pathway for the diversification of this family might be based

[6] Specifically, using the dehalogenase active site as our template, we speculate that the Ser residue (hydrolase Ser138 and synthase Ser161) located on segment 3, position j, may orchestrate proton movement at C(2). 2-Ketocyclohexanecarboxyl-CoA hydrolase additionally contains Glu86 and His89 at positions j and m of segment 4 and His71 at position l of segment 2. These residues may function in the activation of the water ligand and the C═O of the substrate ligand during the addition step. The dihydroxynaphthoate synthase is equipped with a conserved Arg91 at segment 2, position l, and a conserved Gln112 at position m of segment 4 to carry out the reverse of the hydrolase reaction (the His104 residue at segment 4, position e, is not stringently conserved). For both enzymes, the substrate thioester C═O polarization is expected to occur as normal, with Gly66 and Gly110 of segment 2, position g, and Gly86 and Gly133 of segment 1, position b, providing the backbone amide NH H-bonds from the hydrolase and synthase, respectively.

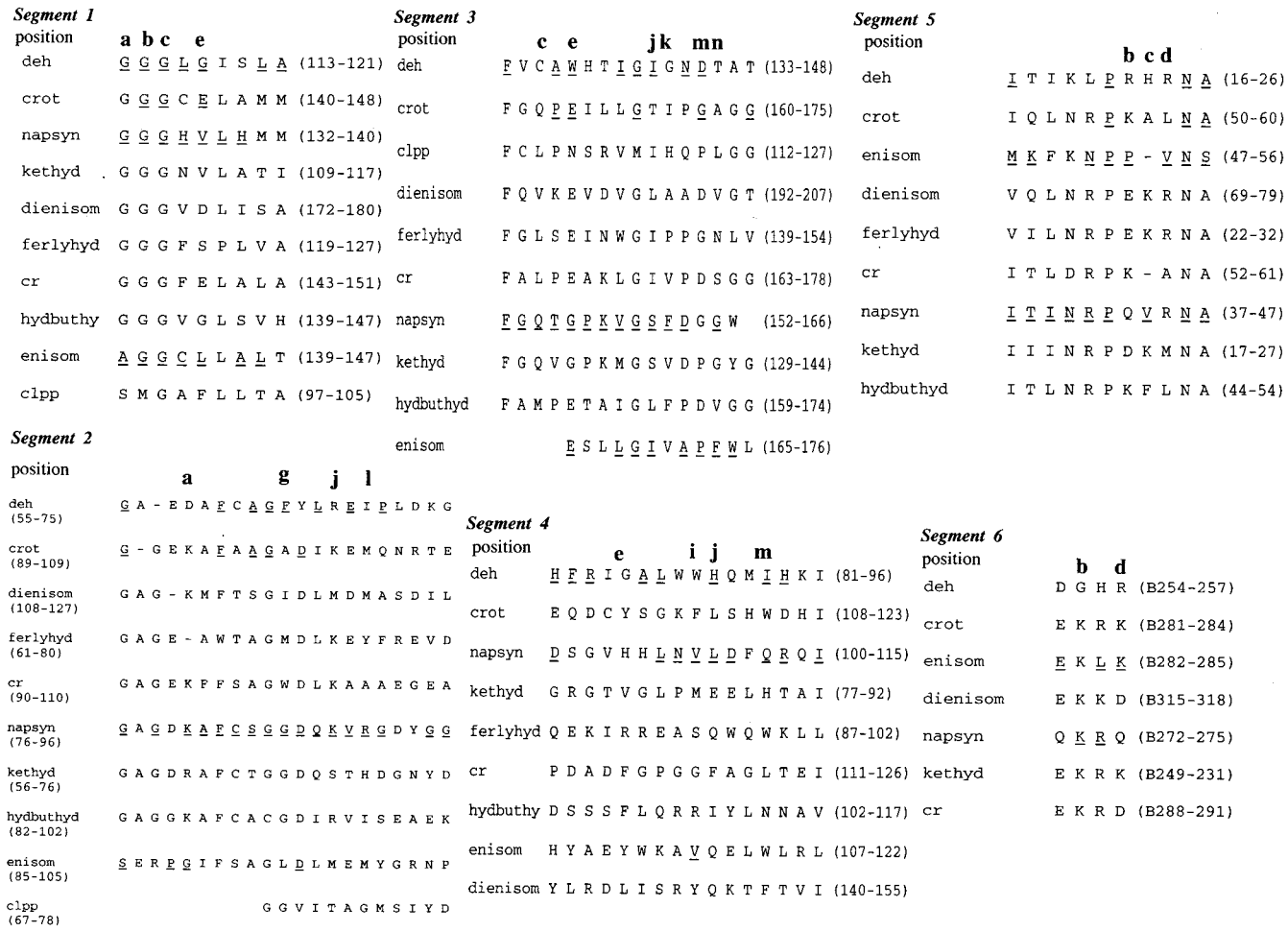

FIGURE 7: Comparison of the sequences of the 2-enoyl-CoA family members in the active site regions (segments 1−6) shown in Figure 5 for 4-CBA-CoA dehalogenase and crotonase. The positions (labeled a, b, c, ...) indicated above the aligned sequences correspond to the positions illustrated for crotonase and 4-CBA-CoA dehalogenase in Figure 5. The residues conserved among subfamilies (eleven crotonase sequences, three 4-CBA-CoA dehalogenase sequences, four dihydroxy-2-naphthoate synthase sequences, and five Δ^3-*cis*,Δ^2-*trans*-enoyl-CoA isomerase sequences) are underlined. The sequence regions shown were taken from a PILEUP (GCG Wisconsin) generated alignment of the following sequences: deh, 4-chlorobenzoyl-CoA dehalogenase, *Pseudomonas* sp. CBS3 (*3*); crot, enoyl-CoA hydratase, *Rattus norvegicus* (mitochondria) (*74*); enisom, rat liver mitochondrial 3,2-*trans*-enoyl-CoA isomerase (*30*); dienisom, rat liver $\Delta^{3,5}$,$\Delta^{2,4}$-dienoyl-CoA isomerase (*75*); ferlyhyd, feruloyl-CoA hydratase/lyase, *Pseudomonas fluorescens* (*25*); cr, carnitine racemase, *R. norvegicus* (*62*); napsyn, 1,4-dihydroxy-2-naphthoate synthase, *E. coli* (*32*); kethyd, 2-ketocyclohexanecarboxyl-CoA hydrolase, *Rhodopseudomonas palustris* (*20*); and hydbuthyd, β-hydroxyisobutyryl-CoA hydrolase, human (*22*).

on strategic placement of one or more polar residues among the stations to perform newly required roles in acid, base, and/or nucleophilic catalysis. The feasibility of this proposal was examined by carrying out the site-directed mutagenesis experiment described in the following section.

Engineering of the 4-CBA-CoA Dehalogenase To Function in the Catalysis of Crotonyl-CoA Hydration. The high similarity observed between the backbone structure of 4-CBA-CoA dehalogenase and that of crotonase provided us with an ideal system with which to examine the feasibility of redirecting the reaction pathway in a progenitor enzyme through minimal changes made in the active site. Our aim was to install the two catalytic Glu residues functioning in crotonase catalysis at the appropriate positions (segment 1, position e, and segment 3, position e; see Figure 5) within the active site of 4-CBA-CoA dehalogenase and determine if the mutant enzyme catalyzes the hydration of crotonyl-CoA to 3-hydroxybutyryl-CoA.

Design of the Crotonase-Active Dehalogenase Mutant. The first step taken was to evaluate wild-type 4-CBA-CoA dehalogenase for its ability to bind crotonyl-CoA, to polarize its thioester C═O, and to add water across its C(2)═C(3). The intrinsic crotonyl-CoA hydratase activity of wild-type 4-CBA-CoA dehalogenase was tested by reacting 65 μM enzyme with 830 μM crotonyl-CoA (pH 7.5, 25 °C). No product was observed following incubation for 14 h, placing an upper limit on the turnover rate of ca. 1×10^{-6} s^{-1}. The K_i values of crotonyl-CoA and the highly chromophoric analogue, acetoacetyl-CoA, were determined to be 1.2 and 0.04 μM, respectively. These K_i values compare well with the $K_m = 40$ μM for crotonase-catalyzed crotonyl-CoA hydration and the $K_i = 1.6$ μM for crotonase inhibition by acetoacetyl-CoA (*30*). Wild-type dehalogenase thus binds the crotonase substrate and inhibitor quite effectively even though it does not catalyze the hydration reaction in the former.

The ability of 4-CBA-CoA dehalogenase and crotonase to polarize the thioester C═O in benzoyl-CoA and in highly conjugated 2-enoyl-CoA substrate analogues, respectively, has been well documented by ^{13}C NMR, UV−visible absorption, and Raman spectral studies of the enzyme-bound ligands (*33*−*36*). Since thioester C═O polarization is

considered to be a prerequisite to catalysis by both enzymes, the ability of the dehalogenase to polarize the thioester C═O in the crotonase substrate and inhibitor was evaluated by measuring the red shift in the ligand thioester C═O absorption band resulting from the transfer of ligand from buffered solution to the enzyme active site. The UV−visible difference spectrum measured for the wild-type dehalogenase−crotonyl-CoA complex revealed a peak at 280 nm having a $\Delta\epsilon = 2.8$ mM^{-1} cm^{-1}. *S*-Crotonyl-*N*-acetylcysteamine displays a λ_{max} at 225 nm ($\epsilon = 10.6$ mM^{-1} cm^{-1}) and at 263 nm ($\epsilon = 6.5$ mM^{-1} cm^{-1}) (*37*). The 17 nm red shift observed in the 263 nm enoyl-thioester absorption band, upon crotonyl-CoA binding to the dehalogenase active site, is indicative of thioester C═O polarization. The polarizing abilities of crotonase and 4-CBA-CoA dehalogenase were compared by determining the magnitudes of the red shifts induced in the inhibitor, acetoacetyl-CoA. The UV−visible absorbance spectrum of acetoacetyl-CoA shows a peak centered at 260 nm ($\epsilon = 15.4$ mM^{-1} cm^{-1}) derived from overlapping absorption bands from the CoA adenine ring and the conjugated thioester moiety. The latter absorption band is shifted to 307 nm ($\Delta\epsilon = 21.6$ mM^{-1} cm^{-1}) when the acetoacetyl-CoA binds to the crotonase active site. The UV−visible difference spectrum of acetoacetyl-CoA complexed to wild-type dehalogenase shows maximum absorbance at 312 nm ($\Delta\epsilon = 21.6$ mM^{-1} cm^{-1}). The observed 52 nm vs 47 nm red shift suggests that the thioester C═O in acetoacetyl-CoA is indeed polarized.

On the basis of the above results we concluded that wild-type dehalogenase can bind and activate crotonyl-CoA for hydration as effectively as crotonase. The active site components needed for crotonyl-CoA turnover were thus narrowed down to the acid (Glu164) and base (Glu144) residues used by crotonase to add the water molecule across the ligand C(2)═C(3). To determine where in the dehalogenase active site the two Glu residues could be most effectively positioned for crotonyl-CoA hydration, the active sites of the dehalogenase and crotonase were superimposed using the backbone of segment 1 (Gly114−Ala121 dehalogenase and Gly141−Met148 crotonase; see Figure 5) as the point of coincidence. In Figure 8, the orientations of the crotonase catalytic groups (Glu 144, Glu 164, Gly141, and Ala 98) relative the corresponding positions (Gly 117, Trp 137, Gly114, and Phe 64) in the dehalogenase active site are shown. On the basis of the overlaid active site structures, substitution of Glu at positions 137 (segment 3, position e) and 117 (segment 1, position e) in the dehalogenase should position the two carboxylate residues for proper orientation of the water molecule for addition across the crotonyl-CoA C(2)═C(3). Given the large size of the Trp residue at position 137, we were confident that the dehalogenase active site could accommodate a Glu side chain at this position. In contrast, the substitution of Glu at Gly117 may cause folding problems that result from unfavorable steric and electronic interactions with the Thr146 and Asp145 residues located on segment 3. Figure 9 illustrates the interaction of the crotonase Glu144 (of segment 1) with the highly conserved segment 3 region (viz., Pro at position l, Gly at position m, and Gly at position p is strictly adhered to, and Ala at position n and Gly at position o is preferred within the crotonase subfamily). Note the favorable packing as well as the use of the backbone NH H-bonds donated from Gly175 and Ala 173 on the loop

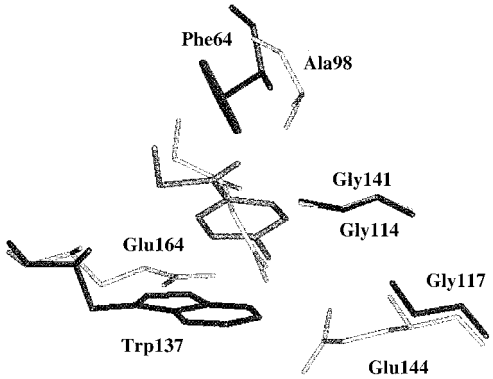

FIGURE 8: Active site residues of 4-CBA-CoA dehalogenase (Trp137, Gly117, and Phe64) superimposed with the active site residues of crotonase (Glu164, Glu144, and Ala98) using segment 1 (Gly114−Ala121 dehalogenase; Gly141−Met148 crotonase) as the point of coincidence. The figure was generated using the X-ray coordinates from the X-ray crystal structures of (rat) crotonase complexed with the inhibitor acetoacetyl-CoA (*30*) and (*Pseudomonas*) 4-CBA-CoA dehalogenase complexed with its product ligand 4-HBA-CoA (*29*) and the software package InsightII. The benzoyl moiety of the 4-HBA-CoA ligand and the acetoacetyl moiety of the acetoacetyl-CoA ligand are featured in the center of the figure.

to orient the Glu carboxylate for catalysis. Unfortunately, the 4-CBA-CoA dehalogenase segment 3 residues are comparatively bulky, a structural feature compatible with the small side chain of Gly117 on segment 1 but not, as shown in Figure 9, compatible with the large, charged Glu side chain found in crotonase. Indeed, the insolubility of the dehalogenase G117E mutant prompted us to substitute all five residues (171PGAGG175) of the crotonase segment 3 region for the corresponding residues (144NDTAT148) in the dehalogenase. In addition, we noticed from the aligned crotonase sequences that proline is stringently conserved at segment 3, position d. We suspected that this proline serves in crotonase catalysis to help to orient the catalytic side chain of the neighboring Glu164 (segment 3, position e). Consequently, we also included our design of the dehalogenase mutant, the substitution of Ala136 with Pro. The resulting mutant, G117E/A136P/W137E/N144P/D145G/T146A/A147G/T148G dehalogenase, contains eight amino acid substitutions. We note that five out of the eight amino acid substitutions made may have been unnecessary if we were to start with a progenitor having the trim segment 3, characteristic of the crotonase subfamily and several other family members [see the compilation of sequences provided in Wu et al. (*31*)]. Likewise, a more suitable progenitor would have a Pro residue preceding the catalytic Glu, as observed in four other members of the 2-enoyl-CoA family (*38*−*41*).

Rate and Stereochemistry of Crotonyl-CoA Hydration Catalyzed by the G117E/A136P/W137E/N144P/D145G/T146A/A147G/T148G Dehalogenase Mutant. The crotonyl-CoA hydration activity of this dehalogenase mutant was measured using a discontinuous HPLC-based assay (in which the product ligand, 3-hydroxybutyryl-CoA, was separated and quantitated) and a continuous spectrophotometric-based assay (in which crotonyl-CoA hydration was monitored by the decrease in absorbance at 280 nm, $\Delta\epsilon = 3600$ M^{-1} cm^{-1}). The k_{cat} determined from a steady-state initial velocity study of the crotonyl-CoA hydration reaction using the spectrophotometric assay is 0.064 ± 0.003 s^{-1} and the $K_m = 51.0 \pm 0.6$ μM. For comparison, the k_{cat} for wild-type dehaloge-

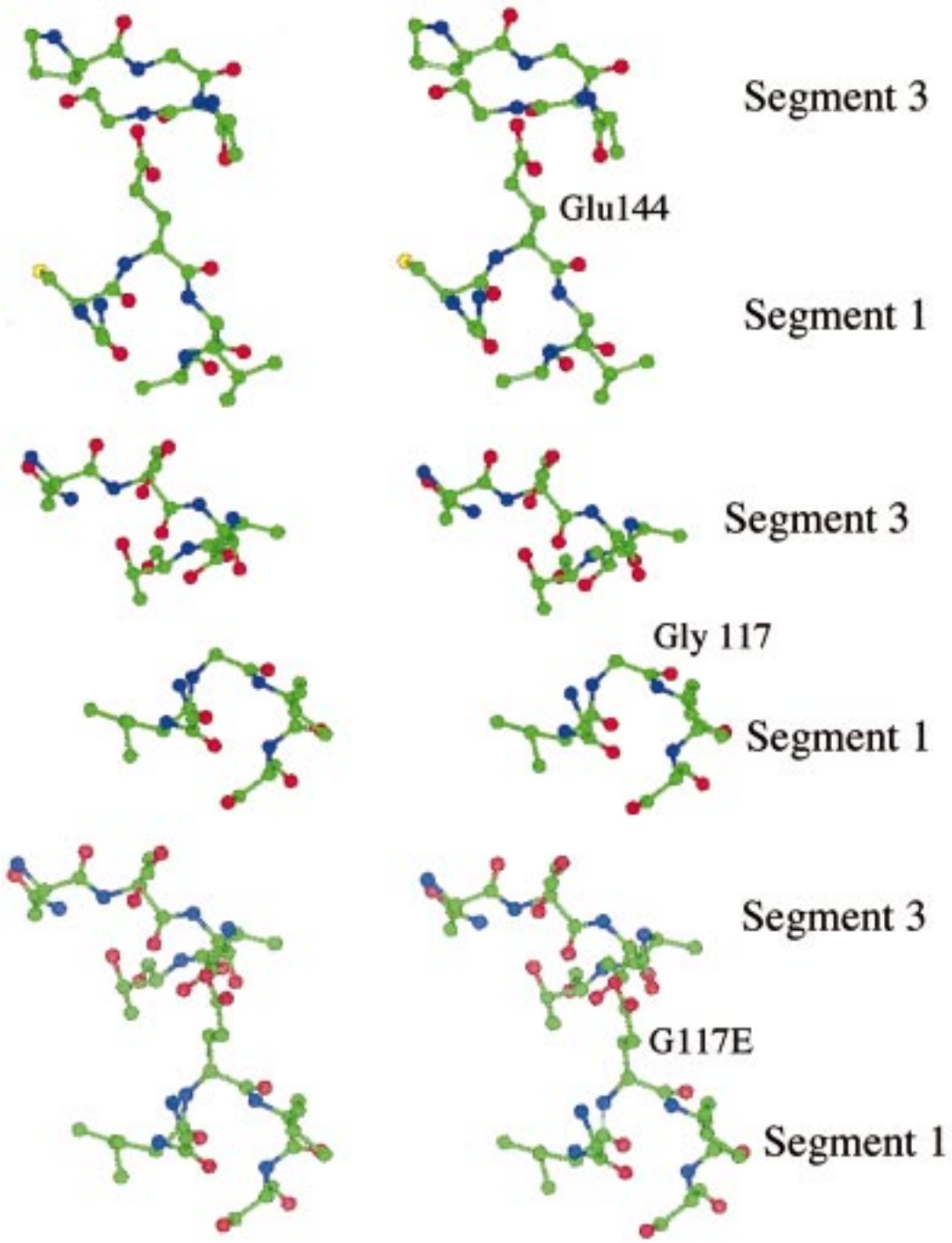

FIGURE 9: Stereoview comparison of the side chain packing between the loop region of segment 3 (171PGAGG175) and segment 1 (143CELAM147) of crotonase (top) and between the loop region of segment 3 (144NDTAT148) and segment 1 (116LGISL120) of 4-CBA-CoA dehalogenase (middle). The figure was generated using the X-ray coordinates from the X-ray crystal structures of (rat) crotonase complexed with the inhibitor acetoacetyl-CoA (*30*) and (*Pseudomonas*) 4-CBA-CoA dehalogenase complexed with its product ligand 4-HBA-CoA (*29*) and the software package InsightII. The two structures were first superimposed using the N-terminus of helix 1 (dehalogenase residues 113−115 and crotonase residues 140−143) as the point of coincidence and then separated for side-by-side comparison. The bottom figure shows the loop region of segment 3 (144NDTAT148) and segment 1 (116LEISL120) of a mutant 4-CBA-CoA dehalogenase wherein the Gly117 has been replaced by Glu.

nase-catalyzed dehalogenation of 4-CBA-CoA is 0.6 s^{-1} (K_m = 3 μM) and the k_{cat} for wild-type dehalogenase-catalyzed hydration of crotonyl-CoA is less than 1×10^{-6} s^{-1} (no activity can be detected) while the k_{cat} for crotonase-catalyzed hydration of crotonyl-CoA is 1000 s^{-1} (K_m = 40 μM) (*30*) (see Table 1).

Crotonase-catalyzed hydration of crotonyl-CoA (*trans*-2-butenyl-CoA) proceeds with syn addition of water across the *si* face of the C(2)═C(3) (*42*). The stereochemistry of this reaction is the direct result of the positioning of the two catalytic Glu residues relative to the bound substrate as the anti addition is the predominant pathway observed for the hydroxide-catalyzed reaction in water (*43*). We would expect that if the G117E/A136P/W137E/N144P/D145G/T146A/A147G/T148G dehalogenase mutant catalyzes the hydration of crotonyl-CoA using both Glu residues in an analogous active site configuration, the product of the reaction carried out in D_2O solvent would be (2*R*,3*S*)-[2-H,2-D]-3-hydroxy-

Table 1: Steady-State Kinetic Constants Measured for Crotonase and Wild-Type (w.t.) and Mutant 4-CBA-CoA Dehalogenase (deh) Catalyzed Hydration of *trans*-Crotonyl-CoA at pH 7.5, 25 °C[a]

enzyme	k_{cat} (s^{-1})	K_m (or K_i) (μM)
crotonase	1000	40
w.t. deh	no turnover	1.2[b]
G117E/A136P/W137E/N144P/D145G/T146A/A147G/T148G deh	0.064	51
G117E/A136P/W137D/N144P/D145G/T146A/A147G/T148G deh	0.0001	NA[c]
A136P/ W137E/ D145A deh	0.000064	NA
W137E/D145A deh	no turnover	NA

[a] See Experimental Procedures for details. [b] The K_i determined for *trans*-crotonyl-CoA as a competitive inhibitor vs 4-CBA-CoA. [c] Not applicable; the K_m could not be measured owing to low or no catalytic activity.

butyryl-CoA. The stereochemistry of the hydration reaction was established by ^{1}H NMR using the known stereochemistry of crotonase-catalyzed hydration as the probe. As illustrated in Figure 10 (panels A and E), the hydration of crotonyl-CoA in D_2O catalyzed by crotonase and the mutant dehalogenase produces 2-monodeuterio-3-hydroxybutyryl-CoA in an 8:1 equilibrium mixture with unconsumed crotonyl-CoA. The complete ^{1}H NMR spectrum of the *trans*-crotonyl-CoA/3(*S*)-hydroxybutyryl-CoA equilibrium mixture has been published previously (*12*). The chemical shifts of the C(4) protons (1.22 ppm, doublet, 3 protons) and C(2) proton (2.75 ppm, broad doublet, 1 proton) derived from the respective products of the crotonase and mutant dehalogenase generated mixtures are identical; however, since the shifts do appear to be sensitive to the absolute configuration at C(3) or C(2), their coincidence does not allow direct configuration assignment of the mutant dehalogenase generated product. Panel A shows the signal (a doublet) from the C(2)−HS in (2*R*,3*S*)-2-monodeuterio-3-hydroxybutyryl-CoA at 2.75 ppm that integrates (using the triplet at 2.43 ppm assigned to the two pantetheine C6″ backbone hydrogens as an internal standard) as one proton. Panel B shows the signal (a doublet) from the *pro-R* and *pro-S* protons of C(2) in 3(*S*)-hydroxybutyryl-CoA at 2.77 ppm that integrates as two protons. Panel C shows that crotonase catalyzes the exchange of one of the two C(2) protons from 3(*S*)-hydroxybutyryl-CoA. Panel D shows that only 50% of an equal mixture of 3(*S*)-hydroxybutyryl-CoA and 3(*R*)-hydroxybutyryl-CoA undergoes exchange and that only one of the two C(2) protons is exchanged with the D_2O solvent (the integration of the 2.77 doublet corresponds to 1 proton while the integration of the 2.75 ppm doublet corresponds to 0.5 proton). On the basis of these results and the known stereochemistry of the crotonase reaction, we concluded that crotonase-catalyzed deuterium exchange from D_2O will occur only with the C(2)−HR proton in 3(*S*)-hydroxybutyryl-CoA. Panel E shows that the mutant dehalogenase catalyzes the hydration of crotonyl-CoA to 2-monoduetero-3-hydroxybutyryl-CoA. The C(2)−H signal (a doublet) of this product observed at 2.75 ppm integrates as one proton. The spectrum is unchanged when the product is incubated in D_2O containing crotonase (panel F). Panel G shows that incubation of the mutant dehalogenase generated crotonyl-CoA−D_2O hydration product, in H_2O with crotonase, results in the exchange of the C(2)−D to produce C(2)−H_2 (observed as a doublet at 2.77 ppm that integrates as two protons). The spectra represented in panels F and G thus demonstrate that the mutant dehalogenase-catalyzed hydration of *trans*-crotonyl-CoA occurs with syn addition of water across the *si* face of the C(2)═C(3).

Participation of Both Active Site Glu Residues in 8M Dehalogenase Catalysis. The syn stereochemistry observed for G117E/A136P/W137E/N144P/D145G/T146A/A147G/T148G dehalogenase mutant catalyzed crotonyl-CoA hydration suggests that the catalytic Glu residues placed at positions 117 and 137 are both functioning in catalysis. To probe this proposal further, we set out to examine the catalytic properties of mutants in which one of these two Glu residues is replaced with an Ala or Asp residue. Accordingly, three dehalogenase mutants, G117A/A136P/W137E/N144P/D145G/T146A/A147G/T148G dehalogenase, G117D/A136P/W137E/N144P/D145G/T146A/A147G/T148G dehalogenase, and G117E/A136P/W137D/N144P/D145G/T146A/A147G/T148G dehalogenase, were prepared for study. Of these three mutants, only the G117E/A136P/W137D/N144P/D145G/T146A/A147G/T148G dehalogenase mutant proved to be fully soluble and stable. This mutant contains a Glu residue at position 117, but at the other catalytic Glu position, 137, an Asp residue is present. The two negative charges of the original dehalogenase mutant are thus preserved, but the reach of the carboxylate at position 137 has been shortened. The k_{cat} of this mutant, determined using the HPLC method to analyze product formed from the reaction of 30 μM enzyme and 800 μM crotonyl-CoA (pH 7.5, 25 °C), was determined to be 1×10^{-4} s^{-1} (Table 1). The rate contribution of Glu137 is 640-fold larger than that measured for Asp137, suggesting that Glu137 plays a direct role in catalysis of the hydration reaction. The insolubility observed for the G117A/A136P/W137E/N144P/D145G/T146A/A147G/T148G dehalogenase mutant and the G117D/A136P/W137E/N144P/D145G/T146A/A147G/T148G dehalogenase mutant indicated that the mutated loop region of segment 3 (N144P/D145G/T146A/A147G/T148G) is not stable unless combined with a Glu residue at position 117. Thus, to test the catalytic contribution of Glu117 to the G117E/A136P/W137E/N144P/D145G/T146A/A147G/T148G dehalogenase mutant catalyzed crotonyl-CoA hydration, a new mutant, the A136P/ W137E/ D145A dehalogenase mutant, was prepared. This triple mutant is both soluble and stable. The k_{cat} of the A136P/ W137E/ D145A dehalogenase mutant was determined using the HPLC method [to analyze product formed from the reaction of 30 μM enzyme and 800 μM crotonyl-CoA (pH 7.5, 25 °C)] to be 6.4×10^{-5} s^{-1}. Thus, on the basis of the comparison of the k_{cat} for the G117E/A136P/W137E/N144P/D145G/T146A/A147G/T148G dehalogenase mutant (Table 1), the Glu117 appears to make a 1000-fold rate contribution to the catalysis of crotonyl-CoA hydration. When the proline substituted at position 136 is removed (i.e., the proline presumed to function in orienting the Glu residue for catalysis), the

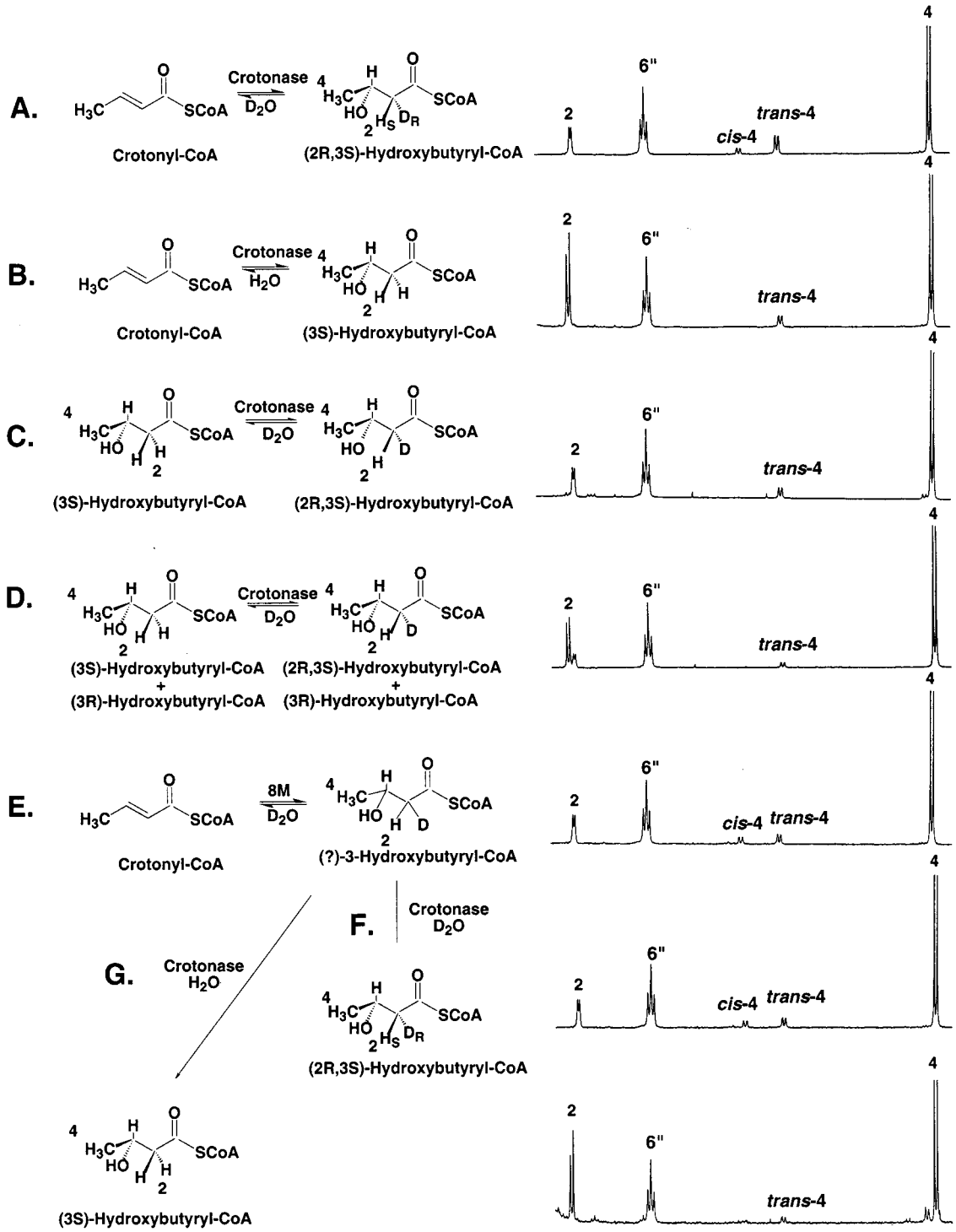

FIGURE 10: ^{1}H NMR (500 MHz) spectra of the equilibrium mixtures of crotonyl-CoA and 3-hydroxybutyryl-CoA generated in H_2O or D_2O (25 °C, D_2O buffered at pD 7.5 with 50 mM phosphate) using crotonase or the G117E/A136P/W137E/N144P/D145G/T146A/A147G/T148G dehalogenase mutant (8M) as catalyst. The C(2) proton(s) and C(4) protons of the predominant component in the mixture, 3-hydroxybutyryl-CoA, are labeled 2 and 4 in the figure, respectively. The signal from the C(4) protons of the trans isomer of crotonyl-CoA is labeled "trans" while the signal from the C(4) protons of the suspected cis isomer (present as a contaminant in the commercial crotonyl-CoA samples) is labeled "cis". The triplet labeled 6" derives from the C(6) protons of the pantenoate moiety of 3-hydroxybutyryl-CoA and crotonyl-CoA.

activity drops below the detection level (1×10^{-6} s^{-1}). While inactive, the double mutant, W137E/D145A dehalogenase, is both soluble and stable. The residual activity observed in the A136P/ W137E/ D145A dehalogenase triple mutant thus appears to derive from the functioning of the Glu at position 137, which is oriented for reaction, in part, by the flanking Pro residue.

Implications for Enzyme Diversification. The pathways of evolution that have produced the enzymes functioning in contemporary organisms are, in the absence of "protein fossils", difficult to trace. Studies of enzyme evolution made through the examination of genetic changes occurring in organisms subjected to lethal or nonlethal selection pressure have provided evidence that practical solutions to survival

typically entail few mutations. Specifically, laboratory-induced bacterial adaptation to novel nutrients commonly involves the enhancement of a minor reaction pathway catalyzed by an enzyme of relaxed substrate specificity [by increased enzyme synthesis via gene duplication or deregulation (*44*, *45*) or by increased catalytic efficiency (*46*−*52*)], if it does not result from the activation of a cryptic gene (*53*−*59*). Enhancements in minor reaction pathways have been observed to occur in enzymes of organisms adapting in nature (the mutation of a cholinesterase in a resistant blow fly to hydrolyze the phosphonate insecticide for example), and they have been achieved by rational active site redesign (the enhancement of nitrile hydrolase activity in papain and asparagine synthetase B for example). The "substrate ambiguity" model (*60*) as revised by Jensen (*61*) may, indeed, account for much of the enzyme diversification that we see today. On the basis of the present work, however, we see that a new enzyme function need not necessarily grow from a minor catalytic pathway existing in a progenitor. An entirely new catalytic pathway can be created at the expense of the preexisting pathway through a limited number of amino acid substitutions, provided that a well-suited progenitor is selected for the job. The catalytic inefficiency (k_{cat} = 0.06 s^{-1}) observed for the "crotonase active" dehalogenase mutant generated in this study is an indication of how far off the dehalogenase active site is from the "ideal" template. At the present we do not know how well the Glu residues at positions 137 and 117 in the dehalogenase mutant are oriented for catalysis nor how well the substrate ligand is oriented for activation by the H-bonds from the backbone amide NHs of Gly114 and Phe64. The determination of the X-ray crystal structure of this mutant (in progress in Hazel Holden's laboratory) should, however, provide significant insight into these questions.

In conclusion, the evolution of the 2-enoyl-CoA family of enzymes from a common active site template could explain how catalytic diversity was achieved by minimal mutation. Although each new enzyme formed in this way would initially be a feeble catalyst, the survival advantage gained from the novel activity would fix the encoding gene so that, over time, additional mutations leading to increased catalytic efficiency might be accumulated.

ACKNOWLEDGMENT

The authors thank Drs. Barry Hall, Vernon Anderson, John Gerlt, Osnat Herzberg, W. W. Cleland, and Hazel Holden for helpful discussions that have taken place during the course of this work and/or during the writing of the manuscript. Dr. Matthew Benning is gratefully acknowledged for his help with the computer graphics and Dr. Yu-Fai Lam for his assistance with the initial NMR experiments. Finally, we thank Dr. Rik Wierenga for providing us with the coordinates of the crotonase X-ray crystal structure.

REFERENCES

1. Babbitt, P. C., and Gerlt, J. A. (1997) *J. Biol. Chem. 272*, 30591−30594.
2. Palosaari, P. M., Vihinen, M., Mantsala, P. I., Alexson, S. E. H., Pihlajaniem, T., and Hiltunen, J. K. (1991) *J. Biol. Chem. 266*, 10750−10753.
3. Babbitt, P. C., Kenyon, G. L., Martin, B. M., Charest, H., Sylvestre, M., Scholten, J. D., Chang, K.-C., Liang, P.-H., and Dunaway-Mariano, D. (1992) *Biochemistry 31*, 5594−5604.
4. Scholten, J. D., Chang, K.-H., Babbitt, P. C., Charest, H., Sylvestre, M., and Dunaway-Mariano, D. (1991) *Science 253*, 182−185.
5. Erlich, H. A., Ed. (1992) *PCR Technology Principles and Applications for DNA Amplification*, W. H. Freeman and Co., New York.
6. Yang, G., Liu, R.-Q., Taylor, K. L., Xiang, H., Price, J., and Dunaway-Mariano, D. (1996) *Biochemistry 35*, 10879−10885.
7. Liang, P.-H., Yang, G., and Dunaway-Mariano, D. (1993) *Biochemistry 32*, 12245−12250.
8. Bahnson, B. J., and Anderson, V. E. (1989) *Biochemistry 28*, 4173−4181.
9. Cleland, W. W. (1979) *Methods Enzymol. 63*, 103−138.
10. Bradford, M. (1976) *Anal. Biochem. 72*, 248−254.
11. Sarma, R. H., and Lee, C. H. (1975) *J. Am. Chem. Soc. 97*, 1225−1236.
12. D'Ordine, R. L., Bahnson, B. J., Tonge, P. J., and Anderson, V. E. (1994) *Biochemistry 33*, 14733−14742.
13. Copley, S. D., and Crooks, G. P. (1994) *Biochemistry 33*, 11645−11649.
14. Loffler, F., Lingins, F., and Muller, R. (1995) *Biodegradation 6*, 203−212.
15. Chang, K.-H., Liang, P.-H., Beck, W., Scholten, J. D., and Dunaway-Mariano, D. (1992) *Biochemistry 31*, 5605−5610.
16. Stern, J. R. (1955) *Methods Enzymol. 1*, 559−556.
17. Kleber, H.-P. (1997) *FEMS Microbiol. Lett. 147*, 1−9.
18. Sharma, V., Suvarna, K., Meganathan, R., and Hudspeth, M. E. S. (1992) *J. Bacteriol. 174*, 5057−5062.
19. Igbavboa, U., and Leistner, E. (1990) *Eur. J. Biochem. 192*, 441−449.
20. Pelletier, D. A., and Harwood, C. S. (1998) *J. Bacteriol. 180*, 2330−2336 .
21. Shimomura, Y., Murakami, T., Fujitsuka, N., Nakai, N., Sato, Y., Sugiyama, S., Shimomura, N., Irwin, J., Hawes, J. W., and Harris, R. A. (1994) *J. Biol. Chem. 269*, 14248−14253.
22. Hawes, J. W., Jaskiewicz, J., Shimomura, Y., Huang, B., Bunting, J., Harper, E. T., and Harris, R. A. (1996) *J. Biol. Chem. 271*, 26430−26434.
23. Stoffel, W., and Grol, M. (1978) *Hoppe Seyler's Z. Physiol. Chem. 359*, 1777−1782.
24. Chen, L.-S., Jin, S.-J., and Tseng, K. Y. (1994) *Biochemistry 33*, 10527−10534.
25. Gasson, M. J., Kitamura, Y., McLauchlan, W. R., Narbad, A., Parr, A. J., Parsons, E. L. H., Payne, J., Rhodes, M. J. C. , and Walton, N. J. (1998) *J. Biol. Chem. 273*, 4163−4170.
26. Maurizi, M. R., Clark, W. P., Katayama, Y., Rudikoff, S., Pumphrey, J., Bowers, B., and Gottesman, S. (1990) *J. Biol. Chem. 265*, 12536−12545.
27. Wang, J., Hartling, J. A., and Flanagan, J. M. (1997) *Cell 91*, 447−456.
28. Modis, Y., Filppula, S. A., Novikov, D. K., Norledge, B., Hiltunen, J. K., and Wierenga, R. K. (1998) *Structure 6*, 957−970.
29. Benning, M. M., Taylor, K. T., Liu, R.-Q., Yang, G., Xiang, H., Wesenberg, G., Dunaway-Mariano, D., and Holden, H. M. (1996) *Biochemistry 35*, 8103−8109.
30. Engel, C. K., Mathieu, M., Zeelen, J. P., Hiltunen, J. K., and Wierenga, R. K. (1996) *EMBO J. 15*, 5135−5145.
31. Wu, W.-J., Anderson, V. E., Raleigh, D. P., and Tonge, P. (1997) *Biochemistry 36*, 2211−2220.
32. Muller-Newen, G., and Stoffel, W. (1993) *Biochemistry 32*, 11405−11412.
33. D'Ordine, R. L., Tonge, P. J., Carey, P. R., and Anderson, V. E. (1994) *Biochemistry 33*, 12635−12643.
34. Taylor, K. L., Liu, R.-Q., Liang, P.-H., Price, J., Dunaway-Mariano, D., Tonge, P. J., Clarkson, J., and Carey, P. R. (1995) *Biochemistry 34*, 13881−13888.
35. Taylor, K. L., Xiang, H., Liu, R.-Q., Yang, G., and Dunaway-Mariano, D. (1997) *Biochemistry 36*, 1349−1361.
36. Clarkson, J., Tonge, P. J., Taylor, K. L., Dunaway-Mariano, D., and Carey, P. (1997) *Biochemistry 36*, 10192−10199.
37. Lynen, F., and Ochoa, S. (1953) *Biochim. Biophys. Acta 12*, 299−304.

38. Zhang, Q. X., and Baldwin, G. S. (1994) *Biochim. Biophys. Acta 1219*, 567−575.
39. Yura, T., Mori, H., Nagai, H., Nakata, T., Ishihama, A., Fujita, N., Isono, K., Mizobuchi, K., and Nakata, A. (1992) *Nucleic Acids Res. 20*, 3305−3308.
40. Preising-Muller, R., Guhnemann-Schafer, K., and Kindl, H. (1994) *J. Biol. Chem. 269*, 20475−20481.
41. Mullany, P., Clayton, C. L., Pallen, M. J., Sloane, R., Al-Saleh, A., and Tabaqchali, S. (1994) *FEMS Microbiol. Lett. 124*, 61−67.
42. Willadsen, P., and Eggerer, H. (1975) *Eur. J. Biochem. 54*, 247−252.
43. Mohrig, J. R., Moerke, K. A., Cloutier, D. L., Lane, B. D., Person, E. C., and Onasch, T. B. (1995) *Science 269*, 527−529.
44. Chen, Y.-M., Chakrabarti, T., and Lin, E., C. (1984) *J. Bacteriol. 159*, 725−729.
45. Rigby, P. W. J., Burleigh, B. D., and Hartley, B. S. (1974) *Nature 251*, 200−204.
46. Pries, F., van den Wijngaard, Bos, R., Pentenga, M., and Janssen, D. B. (1994) *J. Biol. Chem. 269*, 17490−17494.
47. Oliver, E. J., and Mortlock, R. P. (1971) *J. Bacteriol. 108*, 287−292.
48. Wu, T. T., Lin, E. C., and Tanka, S. (1968) *J. Bacteriol. 96*, 447−456.
49. Betz, J. L., Brown, P. R., Smyth, M. J., and Clarke, P. H. (1974) *Nature 247*, 261−264.
50. Hall, B. G. (1977) *J. Bacteriol. 129*, 540−543.
51. Hall, B. G. (1981) *Biochemistry 20*, 4042−4049.
52. Krishnan, S., Hall, B. G., and Sinnot, M. L. (1995) *Biochem. J. 312*, 971−977.
53. Hall, B. G., Yokoyama, S., and Calhoun, D. H. (1983) *Mol. Biol. Evol. 1*, 109−124.
54. Li, W.-H. (1984) *Mol. Biol. Evol. 1*, 212−218.
55. Reynolds, A. E., Felton, J., and Wright, A. (1981) *Nature 293*, 625−629.
56. Hall, B. G. (1998) *Mol. Biol. Evol. 15*, 1−5.
57. Hall, B. G., and Betts, P. W. (1987) *Genetics 115*, 431−439.
58. Paquin, C. E., and Williamson, V. M. (1986) *Mol. Cell Biol. 6*, 70−79.
59. Slater, J. H., Weightman, A. J., and Hall, B. G. (1985) *Mol. Biol. Evol. 2*, 557−567.
60. Horowitz, N. H. (1945) *Proc. Natl. Acad. Sci. U.S.A. 31*, 153−157.
61. Jensen, R. A. (1976) *Annu. Rev. Microbiol. 30*, 409−425.
62. Eichler, K., Bourgis, F., Buchet, A., Kleber, H. P., and Mandrand-Berthelot, M. A. (1994) *Mol. Microbiol. 13*, 775−786.
63. Li, J., Smeland, T. E., and Schulz, H. (1990) *J. Biol. Chem. 265*, 13629−13634.
64. Engel, C. K., Kiema, T. R., Hiltunen, J. K., and Wierenga, R. K. (1998) *J. Mol. Biol. 275*, 847−859.
65. Lai, S.-Y. (1996) Ph.D. Thesis, University of Maryland, Baltimore, MD.
66. Schmitz, A., Gartemann, K.-H., Fiedler, J., Grund, E., and Eichenlaub, R. (1992) *Appl. Environ. Microbiol. 58*, 4068−4073.
67. Kraulis, P. J. (1991) *J. Appl. Crystallogr. 24*, 946−950.
68. Bahnson, B. J., and Anderson, V. E. (1991) *Biochemistry 30*, 5894−5906.
69. Muller, G., Janssen, U., and Stoffel, W. (1995) *Eur. J. Biochem. 228*, 68−73.
70. He, X. Y., and Yang, S.-Y. (1997) *Biochemistry 36*, 1104−11049.
71. Yang, G., Liang, P.-H., and Dunaway-Mariano, D. (1994) *Biochemistry 33*, 8527−8531.
72. Liu, R.-Q., Liang, P.-H., Scholten, J. D., and Dunaway-Mariano, D. (1995) *J. Am. Chem. Soc. 117*, 5003−5004.
73. Luo, M. J., Smeland, T. E., Shoukry, K., and Schulz, H. (1994) *J. Biol. Chem. 269*, 2384−2388.
74. Minami-Ishii, N., Taketani, S., Osumi, T., and Hashimoto, T. (1989) *Eur. J. Biochem. 185*, 73−80.
75. Filppula, S. A., Yagi, A. I., Kilpelainen, S. H., Novikov, D., Fitzpatrick, M., Vihinen, M., Valle, D., and Hiltunen, J. K. (1998) *J. Biol. Chem. 273*, 349−355.

BI9901432